

Feature-based Molecular Networking in the GNPS Analysis Environment

Supplementary information

Louis Felix Nothias,^{1,2,#} Daniel Petras,^{1,2,3,#} Robin Schmid,^{4,#} Kai Dührkop,⁵ Johannes Rainer,⁶ Abinеш Sarvepalli,^{1,2} Ivan Protsyuk,⁷ Madeleine Ernst,^{1,2,8} Hiroshi Tsugawa,^{9,10} Markus Fleischauer,⁵ Fabian Aicheler,^{11,12} Alexander Aksenov,^{1,2} Oliver Alka,^{11,12} Pierre-Marie Allard,¹³ Aiko Barsch,¹⁴ Xavier Cachet,¹⁵ Mauricio Caraballo,^{1,2} Ricardo R. Da Silva,^{2,16} Tam Dang,^{2,17} Neha Garg,¹⁸ Julia M. Gauglitz,^{1,2} Alexey Gurevich,¹⁹ Giorgis Isaac,²⁰ Alan K. Jarmusch,^{1,2} Zdeněk Kameník,²¹ Kyo Bin Kang,^{1,2,22} Nikolas Kessler,¹⁴ Irina Koester,^{1,2,3} Ansgar Korf,⁴ Audrey Le Gouellec,²³ Marcus Ludwig,⁵ Christian Martin H.,²⁴ Laura-Isobel McCall,²⁵ Jonathan McSayles,²⁶ Sven W. Meyer,¹⁴ Hosein Mohimani,²⁷ Mustafa Morsy,²⁸ Oriane Moyne,^{23,29} Steffen Neumann,^{30,31} Heiko Neuweiger,¹⁴ Ngoc Hung Nguyen,^{1,2} Melissa Nothias-Esposito,^{1,2} Julien Paolini,³² Vanessa V. Phelan,³³ Tomáš Pluskal,³⁴ Robert A. Quinn,³⁵ Simon Rogers,³⁶ Bindesh Shrestha,¹⁹ Anupriya Tripathi,^{1,29,37} Justin J.J. van der Hooft,^{1,2,38} Fernando Vargas,^{1,2} Kelly C. Weldon,^{1,2,39} Michael Witting,⁴⁰ Heejung Yang,⁴¹ Zheng Zhang,^{1,2} Florian Zubeil,¹⁴ Oliver Kohlbacher,^{11,12,42,43} Sebastian Böcker,⁵ Theodore Alexandrov,^{1,2,7} Nuno Bandeira,^{1,2,44} Mingxun Wang,^{1,2,44*} and Pieter C. Dorrestein^{1,2,29,39,*}

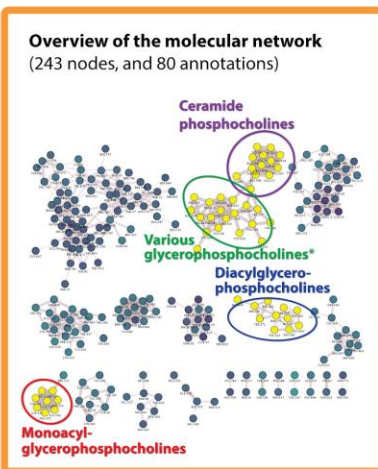
1. Skaggs of Pharmacy and Pharmaceutical Sciences, University of California San Diego, La Jolla, San Diego, CA, USA
2. Collaborative Mass Spectrometry Innovation Center, University of California San Diego, La Jolla, San Diego, CA, USA
3. Scripps Institution of Oceanography, University of California San Diego, La Jolla, CA, USA
4. Institute of Inorganic and Analytical Chemistry, University of Münster, Münster, Germany
5. Chair for Bioinformatics, Friedrich-Schiller-University Jena, Jena, Germany
6. Institute for Biomedicine, Eurac Research, Affiliated Institute of the University of Lübeck, Bolzano, Italy
7. Structural and Computational Biology Unit, European Molecular Biology Laboratory, Heidelberg, Germany
8. Center for Newborn Screening, Department of Congenital Disorders, Statens Serum Institut, Copenhagen, Denmark
9. RIKEN Center for Sustainable Resource Science, Yokohama, Kanagawa, Japan
10. RIKEN Center for Integrative Medical Sciences, Yokohama, Kanagawa, Japan
11. Applied Bioinformatics, Department of Computer Science, University of Tübingen, Tübingen, Germany
12. Institute for Translational Bioinformatics, University Hospital Tübingen, Tübingen, Germany
13. Department of Phytochemistry and Bioactive Natural Products, University of Geneva, Geneva, Switzerland
14. Bruker Daltonics, Bremen, Germany
15. Equipe PNAS, UMR 8038 CiTCoM CNRS, Faculté de Pharmacie de Paris, Université Paris Descartes, Paris, France
16. Department of Physics and Chemistry, School of Pharmaceutical Sciences of Ribeirão Preto, University of São Paulo, Ribeirão Preto, Brazil

17. Technische Universität Berlin, Faculty II Mathematics and Natural Sciences, Institute of Chemistry, Berlin, Germany
18. School of Chemistry and Biochemistry, Center for Microbial Dynamics and Infection, Georgia Institute of Technology, Atlanta, GA, USA
19. Center for Algorithmic Biotechnology, Institute of Translational Biomedicine, St. Petersburg State University, St. Petersburg, Russia
20. Waters Corporation, Milford, MA, USA
21. Institute of Microbiology of the Czech Academy of Sciences, Prague, Czech Republic
22. College of Pharmacy, Sookmyung Women's University, Seoul, Republic of Korea
23. Univ. Grenoble Alpes, CNRS, Grenoble INP, CHU Grenoble Alpes, TIMC-IMAG, Grenoble, France
24. Centro de Biodiversidad y Descubrimiento de Drogas, INDICASAT AIP, Panama, Republic of Panama
25. Department of Chemistry and Biochemistry, Department of Microbiology and Plant Biology and Laboratories of Molecular Anthropology and Microbiome Research, University of Oklahoma, USA
26. Nonlinear Dynamics, Milford, MA, USA
27. Computational Biology Department, School of Computer Sciences, Carnegie Mellon University, Pittsburgh, Pennsylvania, USA
28. Department of Biological and Environmental Sciences, University of West Alabama, Livingston, USA
29. Department of Pediatrics, University of California San Diego, La Jolla, San Diego, CA, USA
30. Bioinformatics and Scientific Data, Leibniz Institute of Plant Biochemistry, Halle, Germany
31. German Centre for Integrative Biodiversity Research (iDiv) Halle-Jena-Leipzig, Germany
32. Laboratoire de Chimie des Produits Naturels, UMR CNRS SPE, Université de Corse Pascal Paoli, France
33. Skaggs School of Pharmacy and Pharmaceutical Sciences, University of Colorado, Denver, Aurora, CO, USA
34. Whitehead Institute for Biomedical Research, Cambridge, MA, USA
35. Department of Biochemistry and Molecular Biology, Michigan State University, East Lansing, 48823, MI, USA
36. School of Computing Science, University of Glasgow, Glasgow G12 8QQ, UK
37. Division of Biological Sciences, University of California San Diego, La Jolla, CA, USA
38. Bioinformatics Group, Wageningen University, Wageningen, the Netherlands
39. Center for Microbiome Innovation, University of California, San Diego, La Jolla, CA, USA
40. Research Unit Analytical BioGeoChemistry, Helmholtz Zentrum München
41. College of Pharmacy, Kangwon National University, Republic of Korea
42. Institute for Bioinformatics and Medical Informatics, University of Tübingen, Tübingen, Germany
43. Biomolecular Interactions, Max Planck Institute for Developmental Biology, Tübingen, Germany
44. Department of Computer Science and Engineering, University of California San Diego, CA, USA

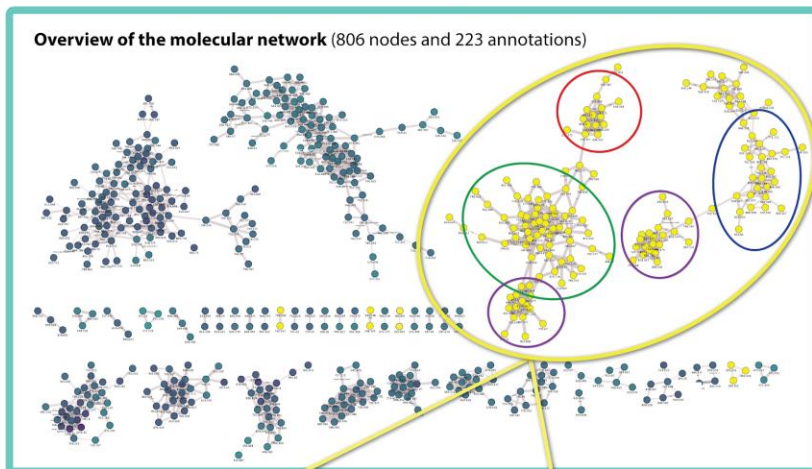
*Correspondence should be addressed to miw023@ucsd.edu or pdorrestein@ucsd.edu

These authors contributed equally

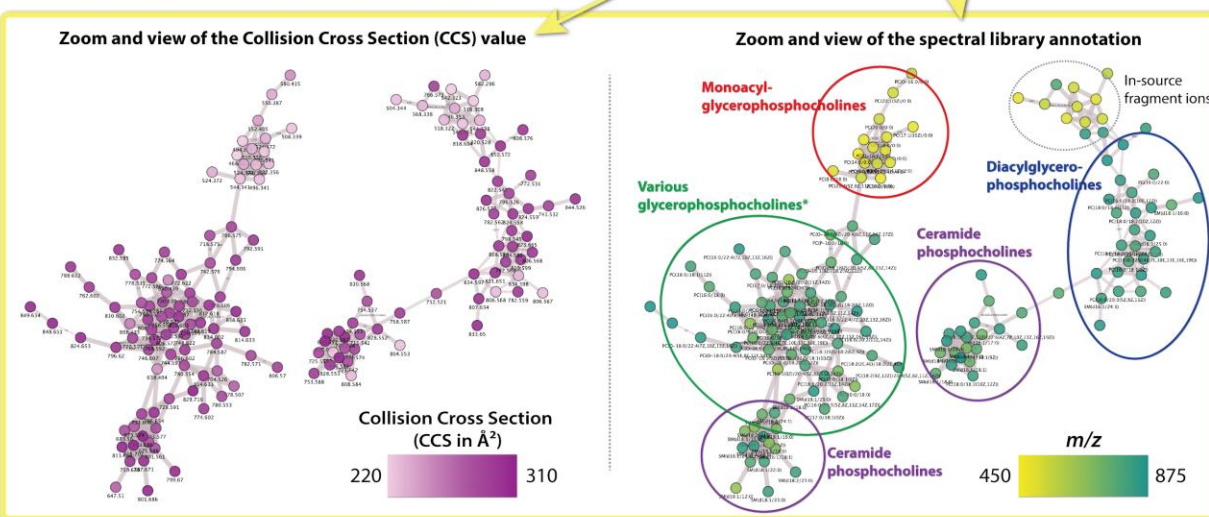
a. Classical Molecular Networking



b. Feature-Based Molecular Networking



c. Phosphatidylcholines molecular networks



Supplementary Figure 1. Analysis of trapped ion mobility spectrometry (TIMS) data of the reference serum sample (NIST 1950 SRM) processed used with Feature-Based Molecular Networking (FBMN) on GNPS. The data were collected on a tims-TOF Pro (Bruker Daltonics, Bremen) in Parallel-Accumulation Serial Fragmentation (PASEF) mode, and processed with MetaboScape. (a) Molecular networks obtained with classical molecular networking; (b) molecular networks obtained with FBMN; and (c) views of the phosphatidylcholine molecular networks with FBMN (the node color gradient to the left shows the cross-collision section value, and the m/z value to the right). Results showed that the use of classical molecular networking drastically reduces the number of nodes (-70%) and spectral annotations (-65%) compared to FBMN. This can be explained by the fact that many isomers are present amongst the lipids annotated (mostly phosphatidylcholines). These isomers tend to produce similar MS² spectra which can be merged by MS-Cluster when performing classical molecular networking. FBMN ensures that the “LC-TIMS-MS” features detected by MetaboScape are preserved which enables the visualization of the Collision Cross Section value in the molecular networks.

Workflow Selection

Search Protocol:

Title:

File Selection

MS2 MGF File: 1 file and 0 folders are selected

Peak Area Quantification Table: 1 file and 0 folders are selected

Sample Metadata: 1 file and 0 folders are selected

Basic Options

Quantification Table Source: XCMS 3

Precursor Ion Mass Tolerance: Da

Fragment Ion Mass Tolerance: Da

Advanced Network Options

Advanced Library Search Options

Advanced Filtering Options

Advanced Quantification Options

Advanced External Tools

Advanced Extras

Workflow Submission

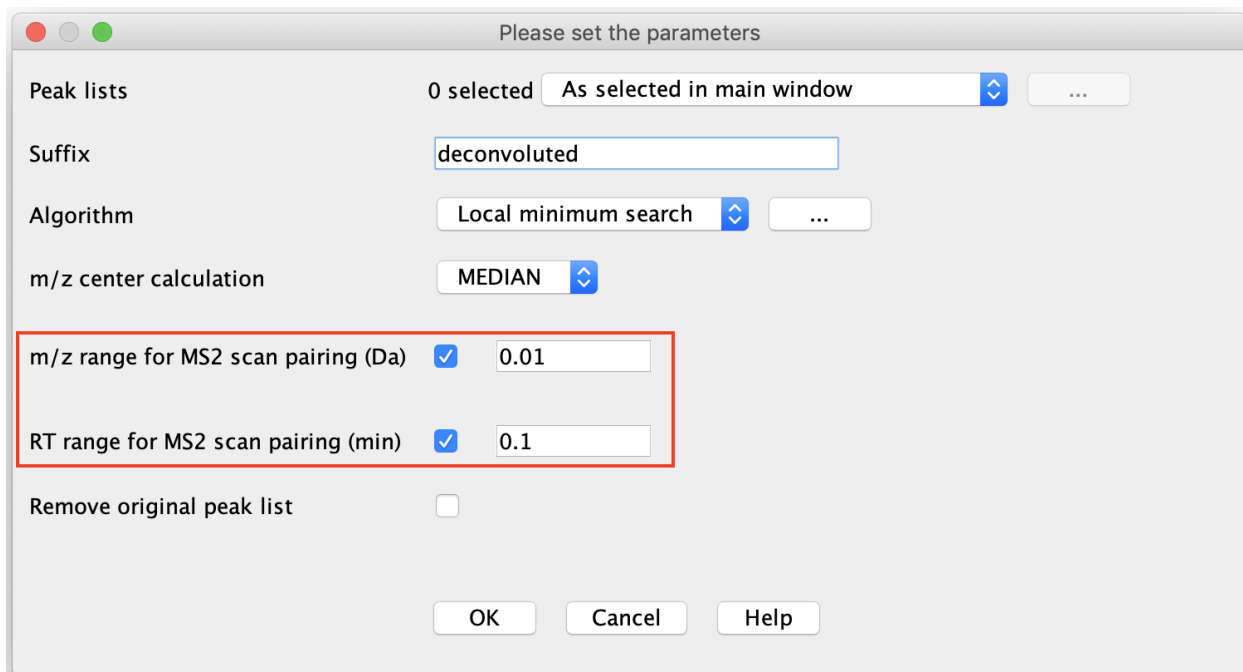
Email me at

Copyright © 2019. Last modified: 2019-07-19. Version 1.3.0-GNPS.

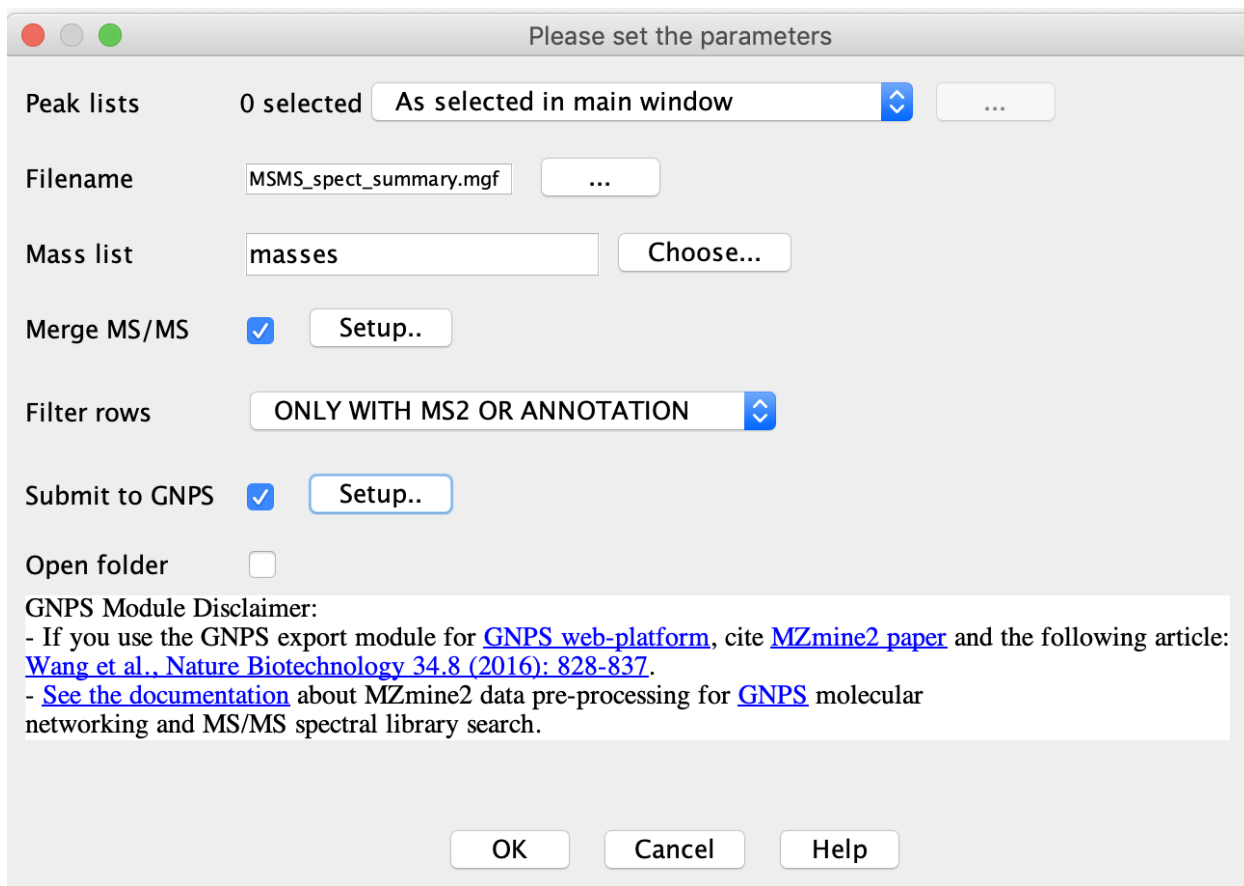
Supplementary Figure 2. Feature-based molecular networking workflow standard interface on GNPS (<https://gnps.ucsd.edu>).

The screenshot displays the web page for Feature-Based Molecular Networking (FBMN) documentation on the GNPS platform. The browser's address bar is highlighted, showing the URL: <https://ccms-ucsd.github.io/GNPSDocumentation/featurebasedmolecularnetworking/>. The page layout includes a navigation sidebar on the left, a main content area, and a table of contents on the right. The main content area provides an introduction to FBMN, lists citations, and details the data processing workflow. The table of contents on the right lists various workflow steps and options, such as 'Introduction', 'Citations', 'Mass Spectrometry Data Processing for the Feature Based Molecular Networking Workflow', 'The Feature Based Molecular Networking Workflow in GNPS', 'Requirement for the FBMN workflow', 'SuperQuick Feature Based Molecular Networking Workflow', 'Running the SuperQuick FBMN', 'Overview of the "standard" Feature Based Molecular Networking Workflow', 'Select the software used for the LC-MS/MS data processing', 'Molecular Networks Options', 'Basic Options', 'Advanced Molecular Network Options', 'Advanced Spectral Library Search Options', 'Advanced Filtering Options (for Spectra)', 'Advanced quantification options', 'Inspecting the Results of FBMN on GNPS', 'Spectral Library Match and Network Topology Analysis', and 'Web-browser Molecular'.

Supplementary Figure 3. The feature-based molecular networking documentation on GNPS (<https://ccms-ucsd.github.io/GNPSDocumentation/featurebasedmolecularnetworking/>).



Supplementary Figure 4. The *Chromatogram deconvolution* module in MZmine and the options added for the pairing of MS¹ feature and MS² scans available since MZmine 2.27.



Supplementary Figure 5. The *Export for/Submit to GNPS* module interface in MZmine, available since version MZmine 2.37.

Please set the parameters

Meta data file ...

Presets HIGHRES ▾

Job title GNPS job direct submission

Username Ifnothias

Password (unencrypted) ●●●●●●●●

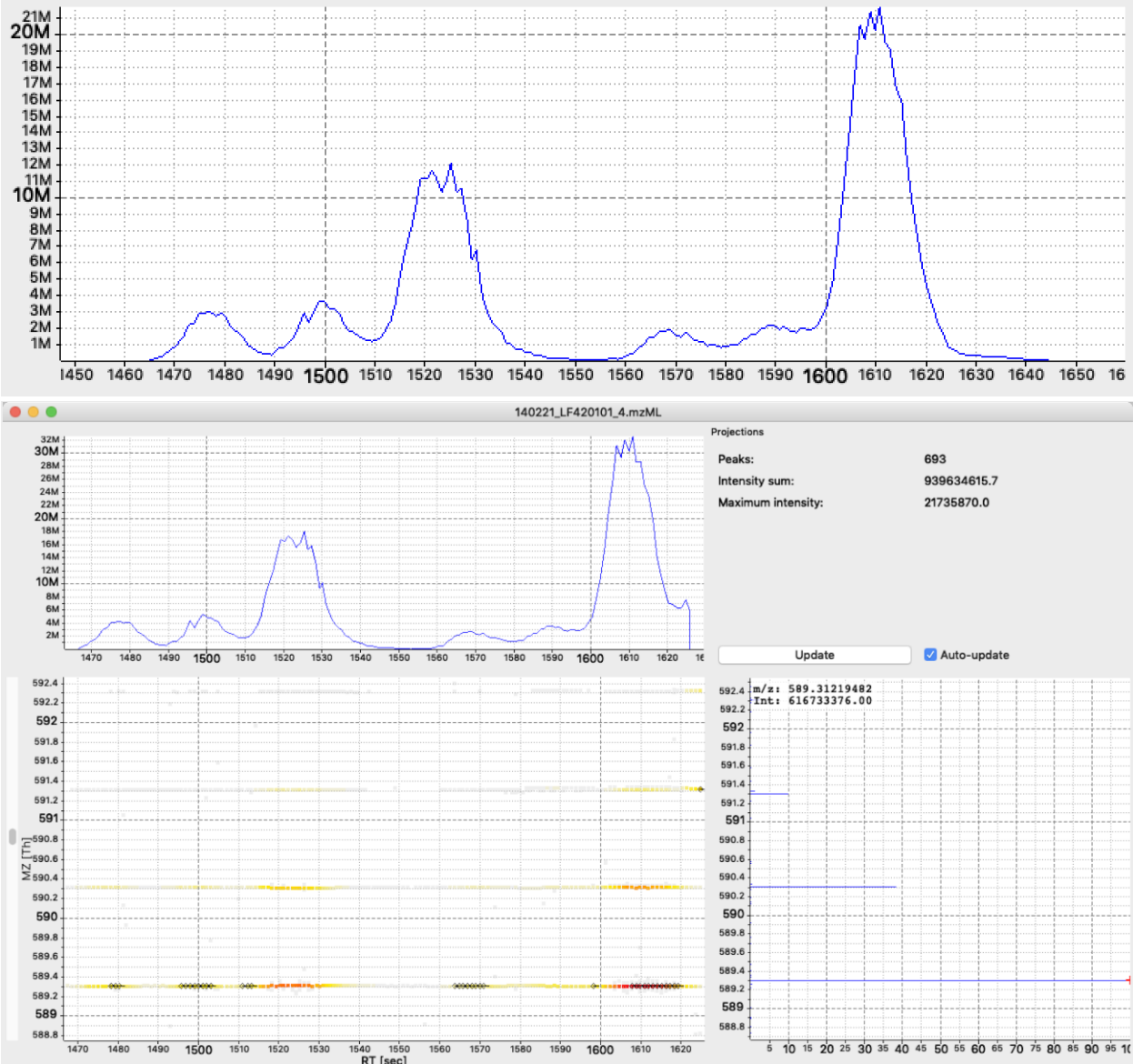
Email nothias@ucsd.edu

Annotation edges

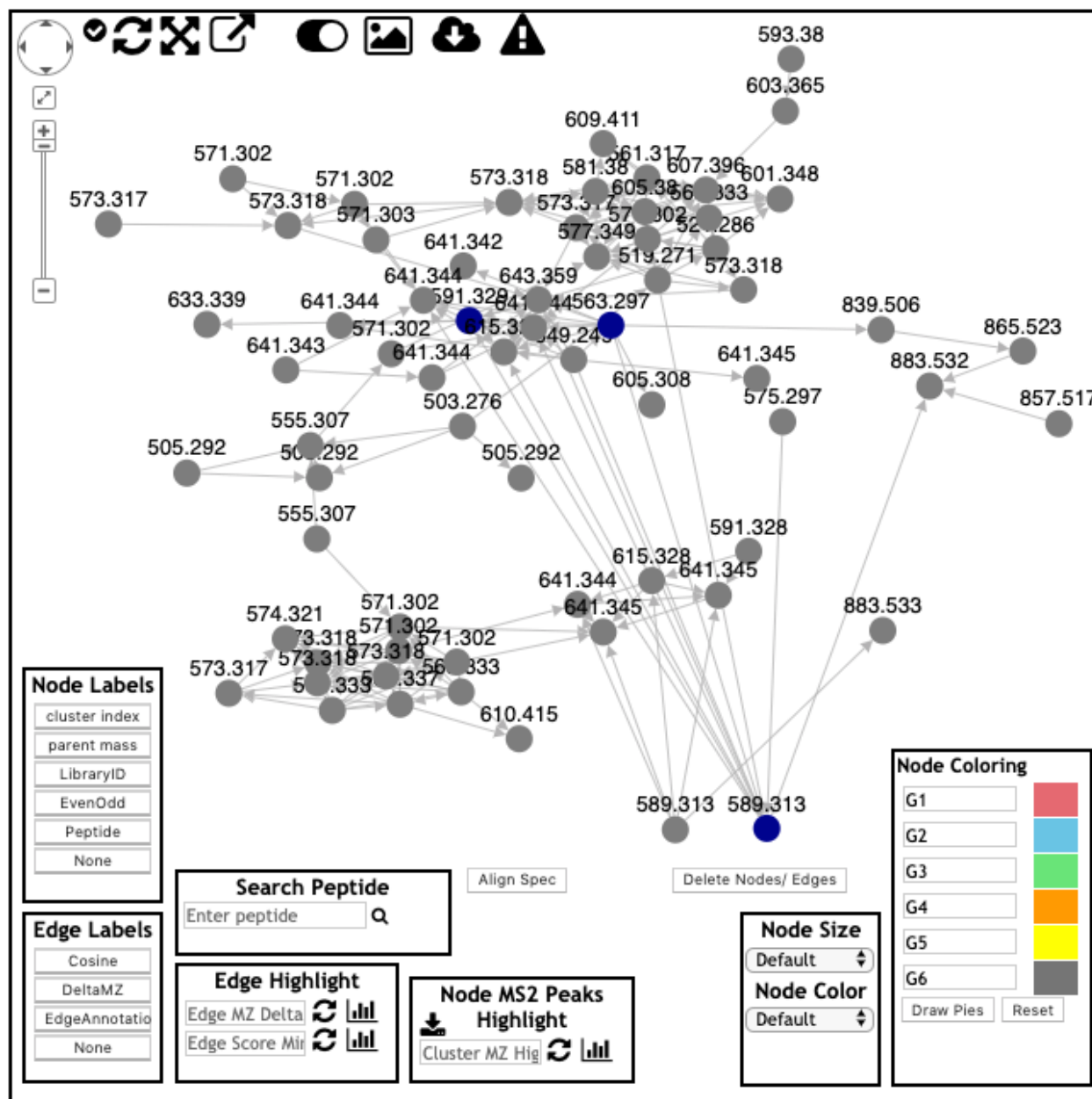
Open website

OK Cancel Help

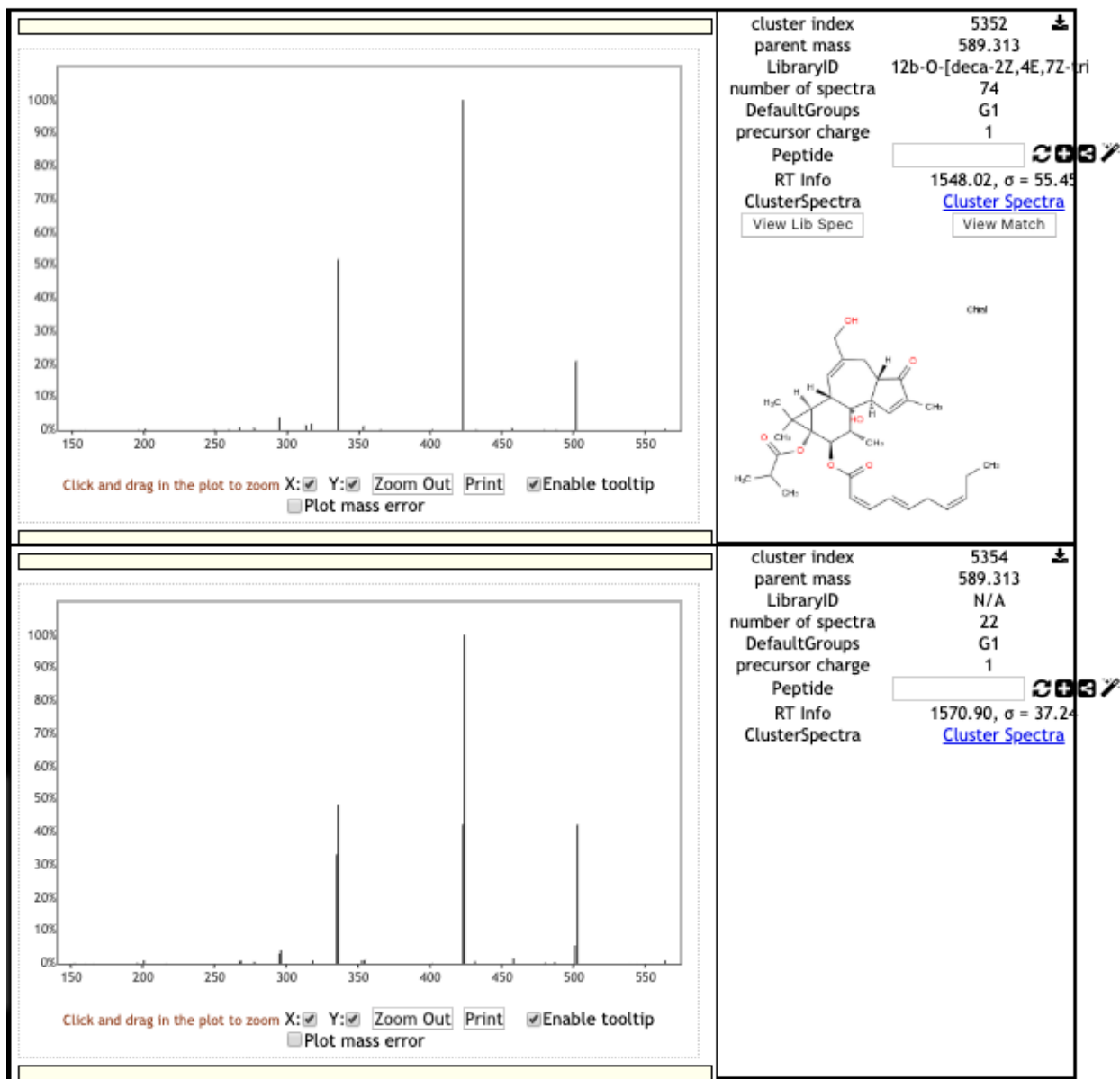
Supplementary Figure 6. Direct submission to GNPS with the *Export for/Submit to GNPS* module in MZmine.



Supplementary Figure 7. Screenshots from OpenMS TOPPView. Top: Extraction Ion Chromatogram (EIC) of m/z 589.31 for the *Euphorbia dendroides* extract (LF420101_4.mzML, $n = 1$ LC-MS² experiment) in the range 1450-1650 seconds. Bottom: Two dimensional LC-MS view of the compounds the isotopic pattern for the m/z 589.31 for the extract of *Euphorbia dendroides*. The top panel shows the EIC for the range m/z 589-592 and 1470-1640 seconds. The lower left panel shows the different intensities per m/z values, and the presence of fragmentation scans (black dots). The right panel shows the full spectrum for the range.

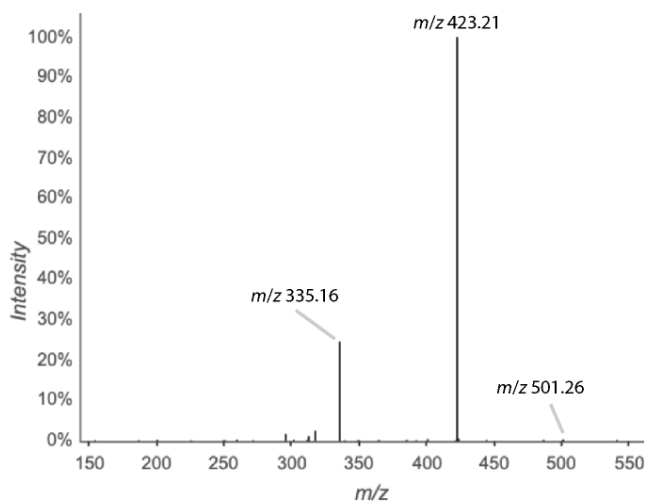


Supplementary Figure 8. [Classical molecular networking](#) analysis of *Euphorbia dendroides* dataset. View of the deoxyphorbol ester molecular network.

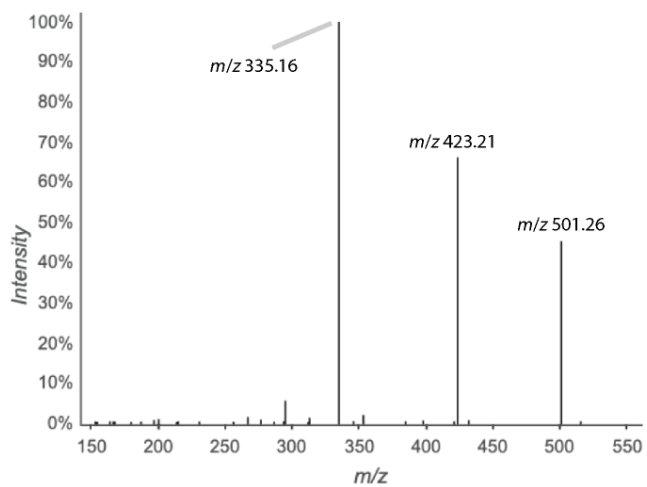


Supplementary Figure 9. [Classical molecular networking](#) analysis of *Euphorbia dendroides* dataset (n = 1 LC-MS² experiment per sample). View of the MS² spectra for the two at m/z 589.313 nodes.

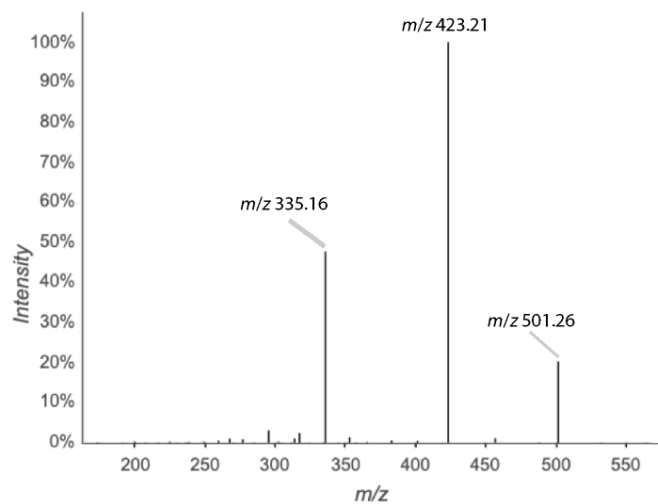
a MS² of *m/z* 589.31 (scan = 2922, ret. time = 1497 sec)



b MS² of *m/z* 589.31 (scan = 3060, ret. time = 1565 sec)



c MS² of *m/z* 589.31 (scan = 3164, ret. time = 1616 sec)



Supplementary Figure 10. Different MS² spectra for the ion m/z 589.31 observed in the *E. dendroides* extract (n = 1 LC-MS² experiment per sample). (a) The first spectral type was observed for the peaks at 24.6 - 25.2 min and characterized by a base peak at m/z 423.21 and a fragment ion m/z 335.16 with 20% relative intensity. (b) The second spectral type was observed for peaks at 26.1 min and a base peak at m/z 335.16, and fragment ions m/z 423.21 and 501.26 with 70-80% and 50-60% of relative intensities, respectively. (c) The third population was found for the chromatographic peaks at 26.1 - 27.0 min with a base peak at m/z 423.21 and fragment ions m/z 335.16 and 501.26 with 35-45% and 15-25% of relative intensities, respectively.

Supplementary Note 1: Detailed discussion about the differences observed between classical molecular networking vs FBMN methods for *Euphorbia dendroides* data.

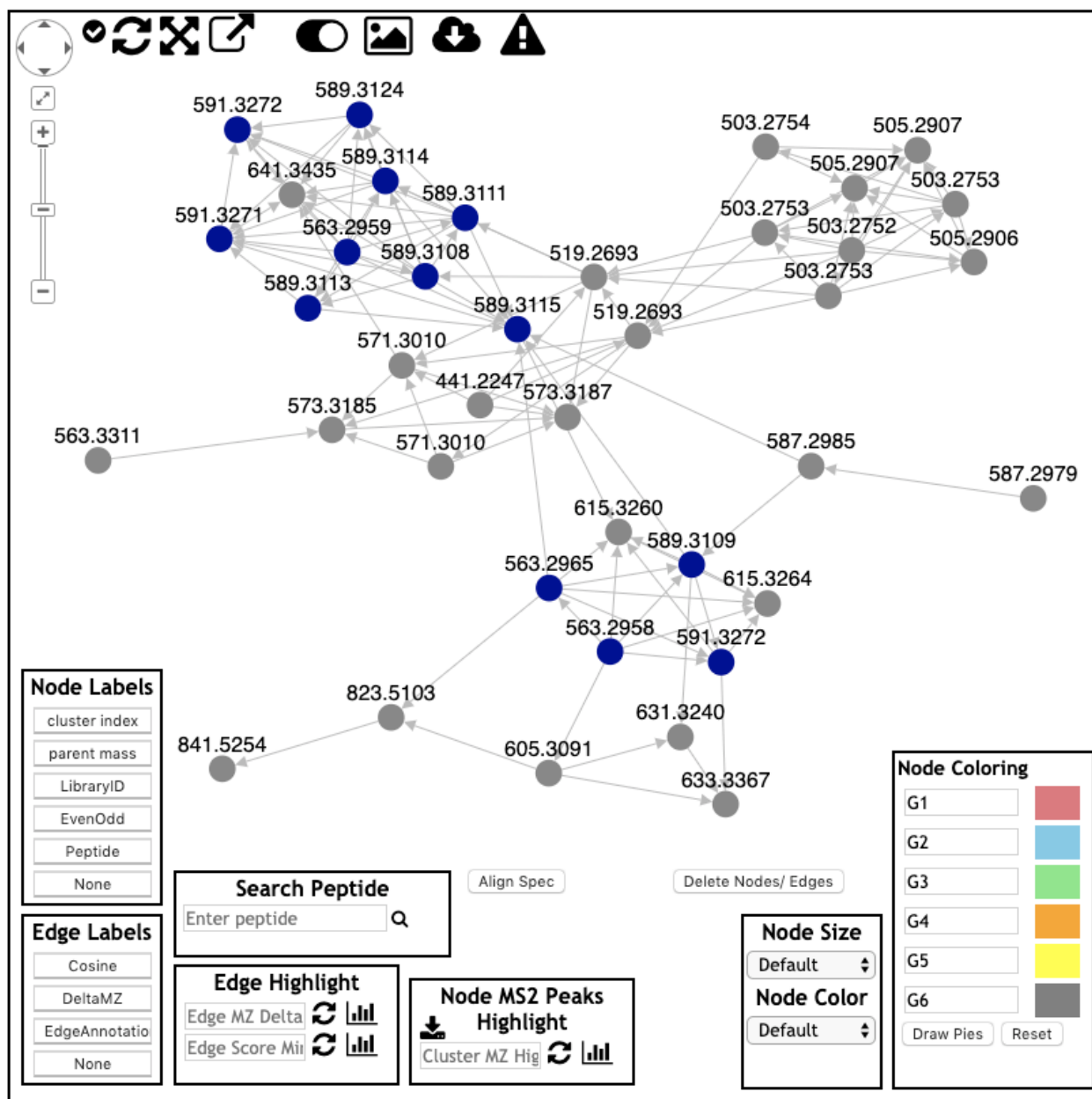
A comparison of results between classical molecular networking vs FBMN (with MZmine) for the *Euphorbia dendroides* dataset is presented in Supplementary Table 1. FBMN is heavily dependent upon user-defined parameters selected during all steps of processing, including peak picking, chromatogram building and deconvolution, isotope grouping, feature alignment and gap filling. The discussion here described differences between the results obtained with classical and FBMN. For the *E. dendroides* dataset processed in MZmine with parameters described in the method, we observed that classical molecular networking produced more network nodes than FBMN. However, FBMN offered a higher spectral annotation rate (5.23%) than classical molecular networking (2.16% with a minimum cluster size = 2). The ratio between unique annotations/total annotations showed that FBMN is capable of separating different isomers, which get merged into one spectrum through the MS-Cluster algorithm in the classical molecular networking workflow (0.42 instead of 0.78 for classical molecular networking). However FBMN was found to provide less unique annotations than classical molecular networking (17 versus 22). This may indicate that relevant features were filtered out during MZmine processing for the FBMN using selected parameters.

MZmine offers various heuristic filters that can be used to reduce the number of features detected. We investigated the results of these filters on the network topology and annotation. When the filters “minimum 2 isotopes detected” and “minimum 2 occurrences” were used for FBMN analysis, the number of nodes became 315 nodes instead of 765 when no filter is used. Moreover, these two filters decreased the proportion of single nodes (31.4% instead of 44.8%), and increased the spectral annotation rate (10.47% instead of 5.23%) which suggests that they efficiently removed low quality spectra. Nevertheless, the use of these filters in MZmine decreased the number of nodes in the molecular network analysis, as seen in the deoxyphorbol molecular family (19 versus 39 nodes without filters). This can be explained by the nature of this dataset, which contains unique spectra from fractions of an *E. dendroides* extract, likely exhibiting high chemical diversity with many unique compounds. Thus, the use of the “minimum 2 occurrences” filter in MZmine, is filtering them out. In addition, the use of the filter “2 minimum isotopes detected” will filter out features that were detected at the limit of detection, and for which no C₁₃ isotopic peak can be observed/paired.

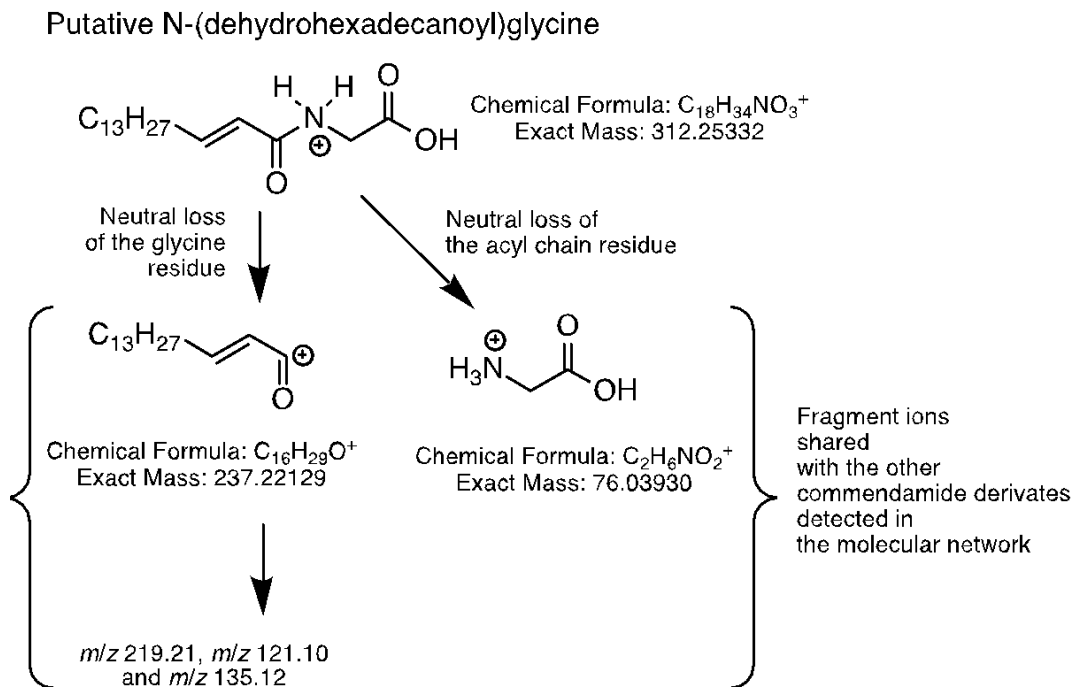
As different parameters selected during MZmine processing affect the final outcome, also the use of different processing software might influence results retrieved. The present FBMN results with MZmine enabled the discrimination of more isomers for the ion m/z 589.311, than when OpenMS was used in the original paper¹, which illustrates how different processing software could lead to different results based on the parameters used and their specificities. In the present case, when using the OpenMS *FeatureFinderMetabo* algorithm, it was observed that closely eluting isomeric features were often detected as a single feature instead of multiple, despite trying various parameters designed to separate features such as the `trace_termination_criteria` (*outlier, sample_rate*).”

Supplementary Table 1. Results for classical molecular networking and feature-based molecular networking (with MZmine) for the *Euphorbia dendroides* dataset.

	Number of nodes	Single nodes	Unique library annotations	Total library annotations	Spectral annotation rate	Size of the deoxyphorbol ester network
Classical molecular networking (minimum cluster size = 2, default)	1,297	519 (40.0%)	22	28	2.16 %	22 (538 total spectra)
Feature based molecular networking without feature filters	765	342 (44.7%)	17	40	5.23 %	39
Feature based molecular networking with feature filter (“minimum 2 isotopes detected”, “minimum 2 occurrences”)	315	98 (31.1%)	15	33	10.47%	19



Supplementary Figure 11. Results of [feature-based molecular networking](#) with MZmine for the *E. dendroides* datasets (n = 1 LC-MS² experiment per sample). View of the entire deoxyphorbol cluster molecular network.



Supplementary Figure 12. Annotation of [\(dehydrohexadecanoyl\)glycine](#), a putative [commendamide derivative](#) in the American Gut Project dataset (dehydrohexadecanoyl)glycine using FBMN on GNPS.

Supplementary Note 2: Protocol for the MassIVE [MSV00008263](#) dataset (EDTA case).

Sample preparation. The 96-well plate PhreeTM Phospholipid Removal Kit was rinsed with 300 μ L of MeOH (100%) and centrifuged at 500 g for 5 min, three times prior to sample addition. Blood plasma was stored at -80°C prior to extraction. The plasma microtubes were thawed at room temperature prior to extraction. Plasma samples were placed randomly into one of two PhreeTM Phospholipid Removal Kit 96-well plates. The thawed plasma samples were vortexed for 5 s and centrifuged for 1 min @ 5000 rpm prior to pipetting 50 μ L of each sample into the 96-well PhreeTM Phospholipid Removal Kit. 200 μ L of MeOH (100%) with 500 ng mL⁻¹ lithocholic acid - d4 as an internal standard was added to each sample well using a multichannel pipette; the solution was aspirated and dispensed five times to mix plasma and organic solvent. 250 μ L of a mixture of the bile acid standards at a concentration of 1000 ng mL⁻¹, individually, in MeOH-Water (4:1) was added to 3 separate well (split 2 on one SPE plate and 1 on the other). A 96-well plate (Eppendorf® Microplate 96/U-PP) was placed under the PhreeTM Phospholipid Removal Kit to collect the sample, and centrifuged at 500 g for 5 min. The PhreeTM Phospholipid Removal Kit portion was discarded and the sample-containing 96-well plate was evaporated until dry using a CentriVap Benchtop Vacuum Concentrator (Labconco, Kansas City, MO, USA). The 96-well plate containing the dried extract were covered (Storage Mat IIITM 3080) and stored at -80°C prior to analysis. Immediately prior to analysis,

the dried extract material was resuspended in 250 μL of MeOH-water (1:1) with 250 ng mL⁻¹ cholic acid - d₄, sonicated for 5 min, centrifuged for 5 min at 500 g, and covered with a plate sealing film (Zone-Free™ Sealing Films).

Data acquisition. Plasma metabolite extracts were analyzed using an ultra-high performance liquid chromatography device (Vanquish, Thermo Fisher Scientific, MA, USA) coupled with an Orbitrap mass spectrometer (Q Exactive, Thermo Fisher Scientific, MA, USA). Chromatographic separation was carried out using a Kinetix C18 1.7 μm , 100 \AA , 50 x 2.1 mm column with corresponding C18 guard cartridge maintained at 40°C during separation. 5.0 μL of extract was injected per sample. Mobile phase composition was as follows: A, water with 0.1% formic acid (v/v) and B, acetonitrile with 0.1% formic acid (v/v). Gradient elution was performed as follows: 0.0, 5.0% B; 1.0, 5.0% B; 1.1, 25.0% B; 5.0, 60.0% B; 5.75, 100.0% B; 6.5, 100%; 6.6, 5.0% B; 7.0, 5.0% B. Flow rate of 0.5 mL min⁻¹ was held constant. Heated electrospray ionization (HESI) was performed in positive ion mode using the following source parameters: spray voltage, 3500 V; capillary temperature, 380 °C, sheath gas, 60.00 (a.u.); auxiliary gas, 20.00 (a.u.); sweep gas, 3.00 (a.u.); probe temperature, 300 °C; and S-lens RF level, 60. The data-dependent acquisition parameters were set as follows: MS1 scans were collected at 30,000 resolution from m/z 150 to 1500 (~7 Hz) with a maximum injection time of 100 ms, 1 microscan, and an automatic gain control target of 1×10^6 . The top 3 most abundant precursor ions in the MS1 scan were selected for fragmentation with an m/z isolation width of 1.5 and subsequently fragmented with stepped normalized collision energy of 20, 30, and 40. The MS2 data was collected at 17,500 resolution with a maximum injection time of 100 ms, 1 microscan, and an automatic gain control target of 5×10^5 .

Supplementary Note 3: FBMN makes it possible to achieve relative quantification

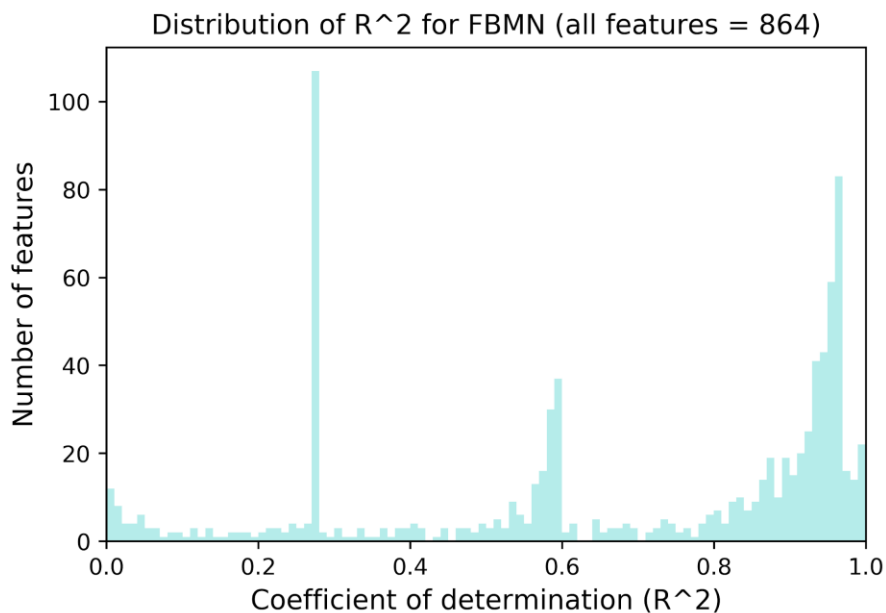
Sample Preparation. The NIST SRM-1950 was prepared and extracted with 80% ethanol as proposed in the SRM 1950 paper².

Mass Spectrometry Analysis. The SRM1950 sample was analyzed using an ultra-high pressure liquid chromatography system (Vanquish, Thermo Fisher Scientific, MA, USA) coupled to an Orbitrap mass spectrometer (Q Exactive, Thermo Fisher Scientific, MA, USA) fitted with a heated electrospray ionization (HESI-II) probe. Chromatographic separation was accomplished using a Kinetex C₁₈ 1.3 μm , 100 \AA , 2.1 mm x 50 mm column fitted with a C18 guard cartridge (Phenomenex) with a flow rate of 0.5 mL/min. 5 μL of extract was injected per sample/QC. The column compartment and autosampler were held at 40°C and 4°C respectively throughout all runs. Mobile phase composition was: A, LC-MS grade water with 0.1 % formic acid (v/v) and B, LC-MS grade acetonitrile with 0.1 % formic acid (v/v). The chromatographic elution gradient was: 0.0 - 1.0 min, 5% B; 1.0 - 9.0 min, 100% B; 9.0 - 11.0 min, 100% B; 11.0 - 11.5 min, 5% B; and 11.5 - 12.5 min, 5% B. Heated electrospray ionization parameters were: spray voltage, 3.5 kV; capillary temperature, 380.0 °C; sheath gas flow rate, 60.0 (arb. units); auxiliary gas flow rate, 20.0 (a. u.); auxiliary gas heater temperature, 300.0 °C; and S-lens RF, 60 (arb. units). MS data was acquired in positive mode using a data dependent method with a

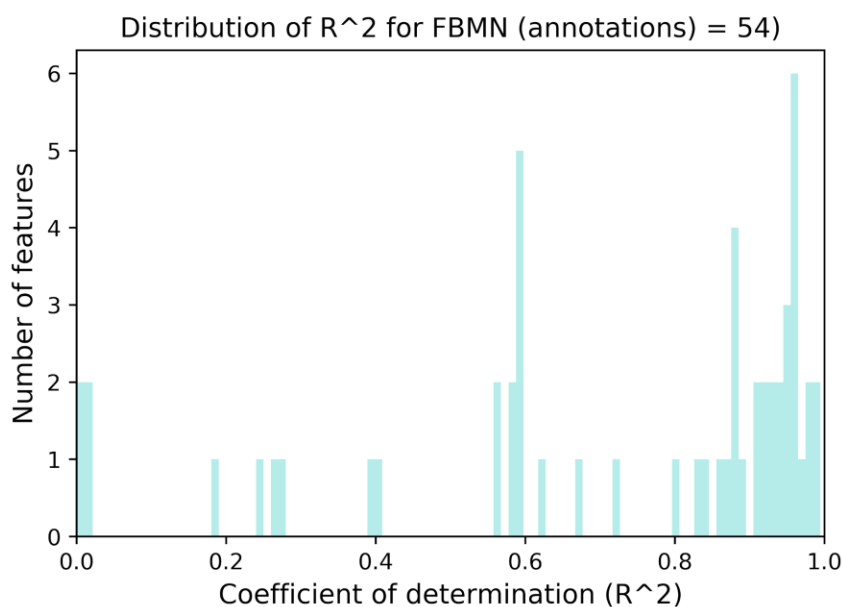
resolution of 35,000 in MS1 and a resolution of 17,000 in MS2. An MS1 scan from 100-1500 m/z was followed by an MS2 scan, using collision induced dissociation, of the five most abundant ions from the prior MS1 scan.

Data interpretation. Classical molecular networking does not use “area under the curve” the relative quantitative information obtained through feature detection of LC-MS traces. The FBMN method brings in ion abundance across all samples by using the value of chromatographic peak areas or peak heights as determined by the LC-MS feature finding software. Using a serial dilution of the NIST 1950 serum reference metabolome sample² analyzed on a Orbitrap instrument (3 LC-MS² independent experiments per sample) and process with MZmine or OpenMS, we show the linearity of the relative quantification capability with FBMN and reveals the improvement compared to classical molecular networking. As mentioned above, the most important limitation of classical molecular networking is the lack of dependable relative quantitative information. The interpretation of non-targeted LC-MS data in metabolomics relies on the statistical analysis of relative variation between ions intensity across the studied samples³. Classical molecular networking uses MS-Cluster results to define the ion distribution between the samples, using either the number of scans clustered in a consensus MS² spectrum (MS² scan table) or the sum of their precursor ion(s) intensities (MS² bucket table). A more accurate comparison of LC-MS data requires the value of chromatographic peak areas (EIC feature) or peak height for each ion features detected and aligned across the samples studied. The FBMN method makes possible to determine the relative intensity of each node in all samples. Using a serial dilution of the NIST 1950 serum reference metabolome sample analyzed on a Q Exactive mass spectrometer⁴, we compared the capability of classical molecular networking and FBMN to evaluate the expected relative ion abundance. After basic optimisation of the software parameters, and as expected for serial dilution, the use of MZmine and OpenMS resulted in feature intensities with high coefficient of determination (R^2) values in Ordinary least squares Linear Regression (OLR) analysis for true positive compounds in the serial dilution samples with a mean R^2 of 0.92 (MZmine, (Figure 2g) and 0.71 (OpenMS, Supplementary Figure 13 and 14), respectively. These differences observed between MZmine and OpenMS processing are partially explained by 1) the lack of a gap-filling step with OpenMS which results in less features detected at the lower concentration range, along with 2) other differences due to the algorithms and parameters used. However, most importantly, the results of classical molecular networking showed that neither the number of MS² scans, or the sum of precursor ion intensity, were able to obtain acceptable coefficient of determination (R^2 mean 0.40 and 0.43, respectively, Supplementary Figures 15 and 17) for all the nodes and the reference compounds (R^2 mean 0.43 and 0.65, respectively, Supplementary Figures 16 and 18). The distribution of the R^2 value showed that ~50% of the features/nodes had a value of 0.33 both using the number of scans (Supplementary Figure 15) or the sum of the precursor ion intensity (Supplementary Figure 17), respectively. The prevalence of that value in both metrics can be explained by the prevalence of ions/features being selected for MS² scans in the most concentrated samples, but not in less concentrated samples. This shows that, while classical molecular networking can be used for

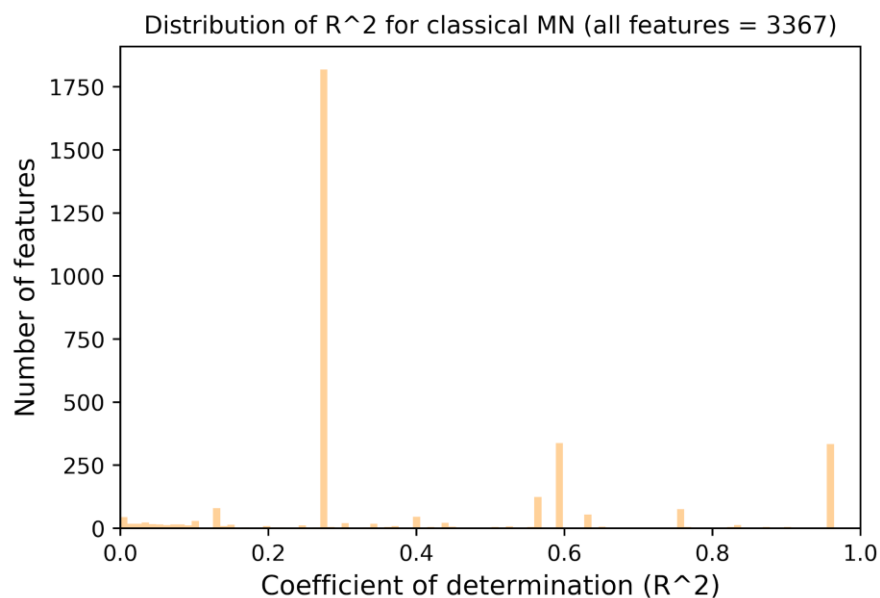
qualitative analysis, and that using the precursor ion intensity appears to perform better than the scan count, it is not suited for accurate ion intensity statistical analysis and that binary metrics (presence/absence) might be better suited to use. Nevertheless, binary interpretation of classical molecular networking should also be considered with caution, as the absence of MS^2 spectra for a compound in one sample does not necessarily mean that the compound was not present, rather than simply below the signal threshold in order to be selected for MS^2 in data-dependent acquisition (DDA) or absent due to other reasons.



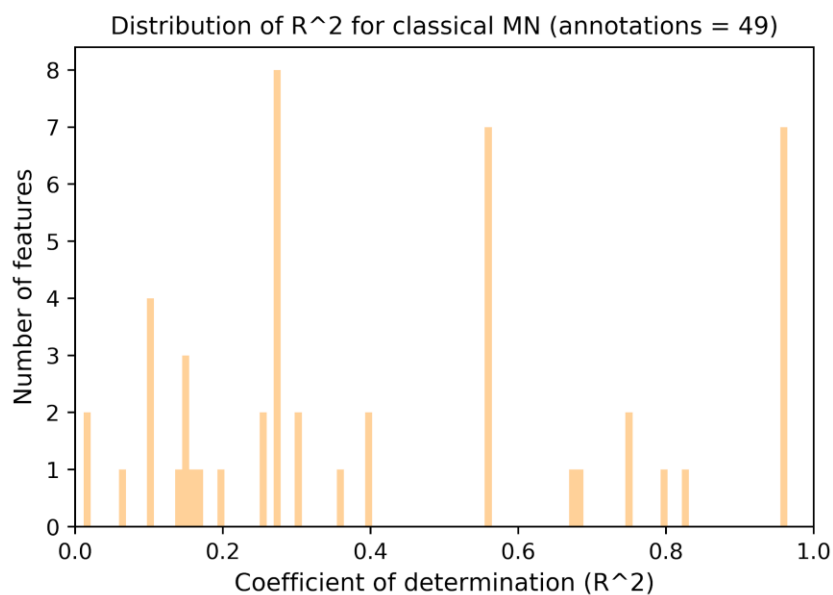
Supplementary Figure 13. Distribution of the coefficient of determination (R^2) from least square regression analysis between the feature intensities ($n = 864$) and the expected relative concentration for a serial dilution analyzed by LC- MS^2 (3 independent experiments per sample) and processed with OpenMS for FBMN.



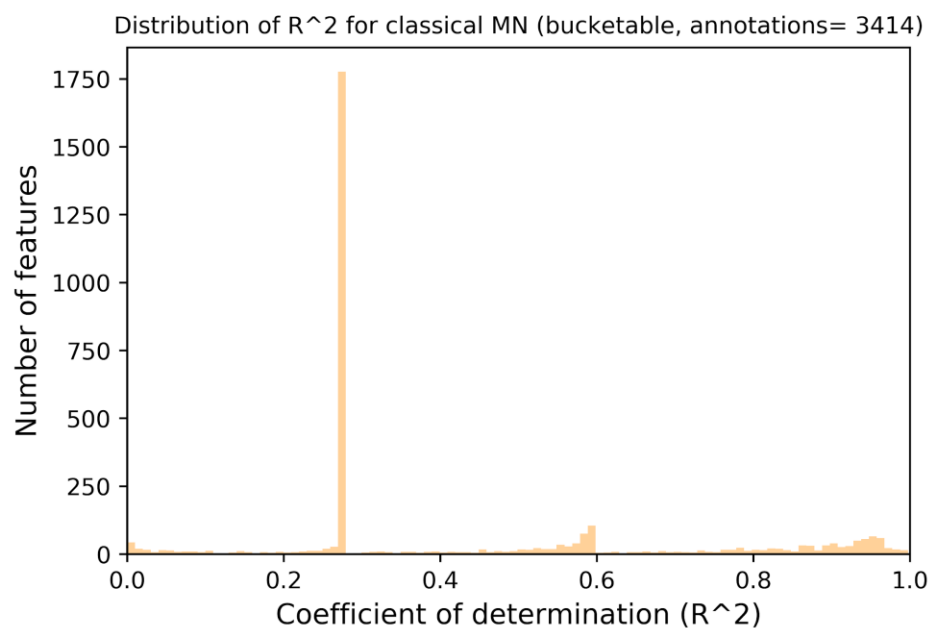
Supplementary Figure 14. Distribution of the coefficient of determination (R^2) from least square regression analysis between the feature intensities of annotated compounds ($n = 54$) and the expected relative concentration for a serial dilution analyzed by LC-MS² (3 independent experiments per sample) and process with OpenMS for FBMN.



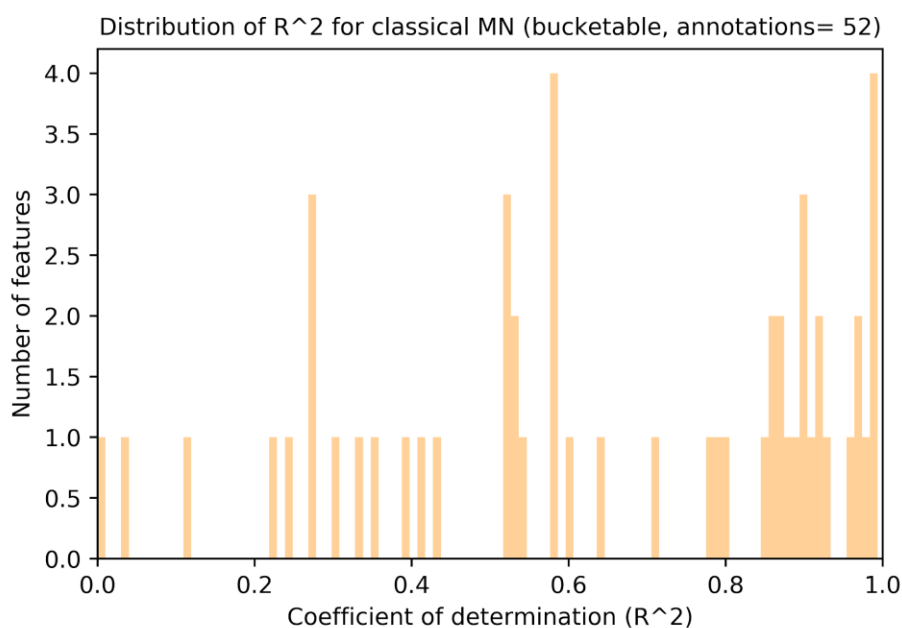
Supplementary Figure 15. Distribution of the coefficient of determination (R^2) from least square regression analysis between the feature (node, $n = 3,367$) spectral count and the expected relative concentration with classical MN for a serial dilution analyzed by LC-MS² (3 independent experiments per sample).



Supplementary Figure 16. Distribution of the coefficient of determination (R^2) from least square regression analysis between the feature (node) spectral counts of annotated compounds ($n = 49$) and the expected relative concentration with classical MN for a serial dilution analyzed by LC-MS² (3 independent experiments per sample).



Supplementary Figure 17. Distribution of the coefficient of determination (R^2) from least square regression analysis between the feature (nodes, $n=3,414$) precursor intensity and the expected relative concentration with classical MN for a serial dilution analyzed by LC-MS² (3 independent experiments per sample).



Supplementary Figure 18. Distribution of the coefficient of determination (R^2) from least square regression analysis between the precursor intensity for the annotated compounds (node, n

= 52) and the expected relative concentration with classical MN for a serial dilution analyzed by LC-MS² (3 independent experiments per sample).

Supplementary Note 4: Large dataset processing with XCMS

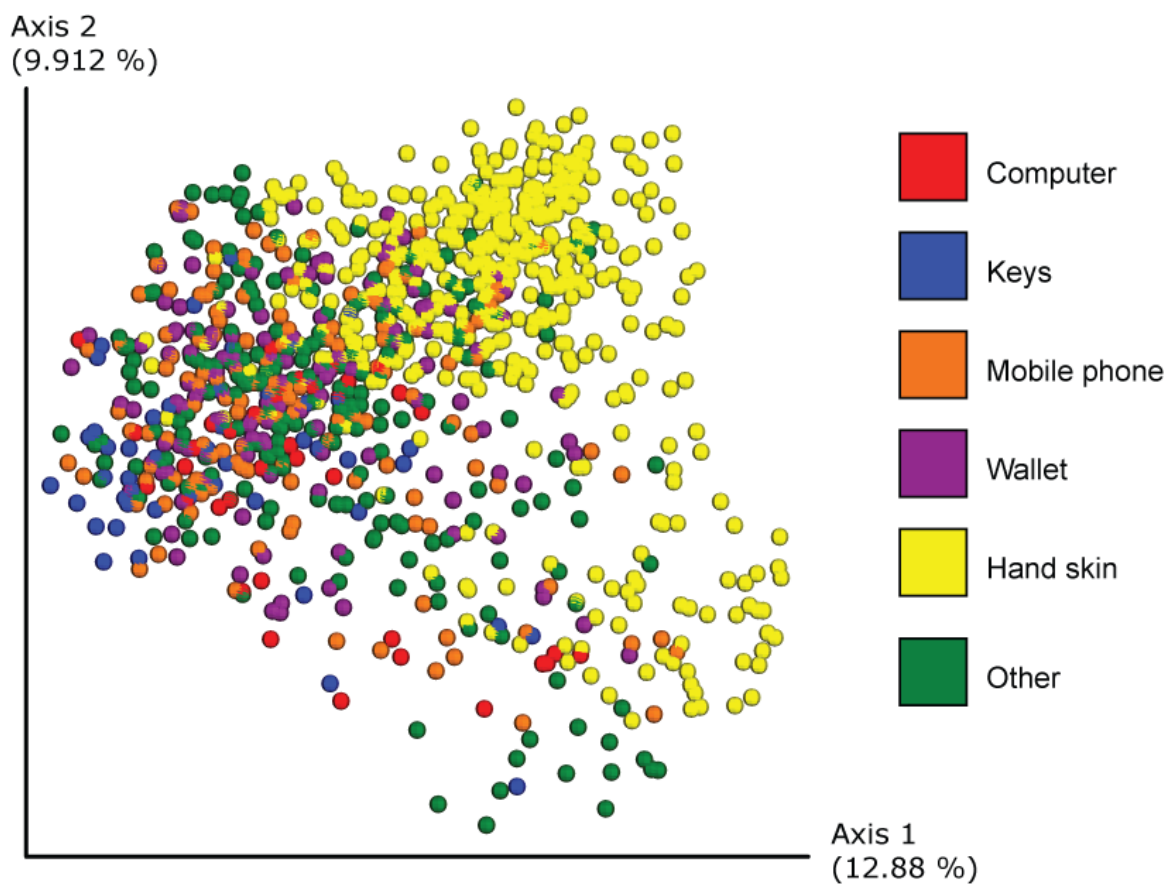
The processing of very large metabolomics dataset (more than a thousand samples) is limited by the scalability of existing LC-MS feature detection tools, especially for those based on graphical user interfaces (such as MZmine and MS-DIAL). MZmine was successfully used for the processing of large datasets acquired on QTOF mass spectrometers, but required both a powerful workstation computer (with 64GB of RAM memory), and the use of sub-optimal parameters, such as higher noise thresholds, to reduce the computational load. Here, we show that XCMS and OpenMS can be used to process large metabolomics studies for FBMN analysis. The MassIVE dataset [MSV000080030](https://massive.ucsd.edu/MSV000080030) consists of approximately 2,000 samples from the forensic study with samples from hands and objects of 80 participants analyzed on a QTOF by LC-MS²⁵. The files were processed with XCMS or OpenMS running on cluster computers. For XCMS, the processing was performed on 8 processors with 32 GB of RAM memory allocated for each process and took 8 hours. The XCMS script is available at https://github.com/DorresteinLaboratory/XCMS3_FeatureBasedMN and the FBMN job on GNPS (<https://gnps.ucsd.edu/ProteoSAFe/status.jsp?task=cf026a37c70946a1a937e030dea65514>, runtime = 6 hours and 20 minutes).

For OpenMS processing, the OpenMS-GNPS workflow was used and run on the CCMS cluster (<https://gnps.ucsd.edu/ProteoSAFe/status.jsp?task=e0a0694c3bcb42969d59354a822f5254#>, runtime = 6 hours and 26 minutes). As observed for FBMN with XCMS, the number of features detected and spectral library matches show that, for large datasets FBMN will result in less annotations (0.7% instead of 1.0% for classical molecular networking, in Supplementary Table 2). Indeed, these feature detection tools were not designed to process multi-thousands files datasets. As a result, the processing of 2,000 files requires sub-optimal parameters (noise level, feature intensity threshold) to limit the computational load, and of heuristic(s) (such as a minimum number of occurrences in the dataset, or the presence of isotopologues) to limit the number of features outputted for downstream analysis. This illustrates the continued need for improvement of LC-MS feature detection on large metabolomics datasets, that will enable sensitive detection within a reasonable runtime.

Supplementary Table 2. Comparison of the results for the MassIVE [MSV000080030](https://massive.ucsd.edu/MSV000080030) dataset (QTOF) including 2000 samples using classical molecular networking and feature-based molecular networking with XCMS.

	Number of features	Single nodes	Unique library annotations	Spectral annotation rate	Runtime for feature detection/alignment	Runtime for molecular

						networking on GNPS
Classical molecular networking	20,578 (nodes)	18,946 (92,1%)	208	1.0 %	Not applicable	11h44min
Feature-based molecular networking with XCMS	13,862 (LC-MS features with MS2)	12,045 (86.9%)	97	0.7 %	6h26min	6h20min



Supplementary Figure 19. Principal Coordinate Analysis of the forensic study ([MSV000080030](#), approximately 2,000 samples, n= 1 LC-MS² experiment per sample) processed with XCMS and analyzed with the FBMN workflow on GNPS. See [this link](#) for an interactive visualization of the plot.

References for Supplementary Information

1. Nothias, L.-F. *et al.* Bioactivity-Based Molecular Networking for the Discovery of Drug Leads in Natural Product Bioassay-Guided Fractionation. *J. Nat. Prod.* **81**, 758–767 (2018).
2. Simón-Manso, Y. *et al.* Metabolite profiling of a NIST Standard Reference Material for human plasma (SRM 1950): GC-MS, LC-MS, NMR, and clinical laboratory analyses, libraries, and web-based resources. *Anal. Chem.* **85**, 11725–11731 (2013).
3. Sugimoto, M., Kawakami, M., Robert, M., Soga, T. & Tomita, M. Bioinformatics Tools for Mass Spectroscopy-Based Metabolomic Data Processing and Analysis. *Curr. Bioinform.* **7**, 96–108 (2012).
4. da Silva, R. R. *et al.* Computational Removal of Undesired Mass Spectral Features Possessing Repeat Units via a Kendrick Mass Filter. *J. Am. Soc. Mass Spectrom.* **30**, 268–277 (2019).
5. Bouslimani, A. *et al.* Lifestyle chemistries from phones for individual profiling. *Proc. Natl. Acad. Sci. U. S. A.* **113**, E7645–E7654 (2016).